Journal of Catalysis **211,** 53–63 (2002)
doi:10.1006/jcat.2002.3746

# Product Analysis of Selective Catalytic Reduction of $NO_2$ with $C_2H_4$ over H–Ferrierite

Tetsuya Nanba,[1] Akira Obuchi, Yousuke Sugiura, Chizu Kouno, Junko Uchisawa, and Satoshi Kushiyama

*Institute for Environmental Management Technology, National Institute of Advanced Industrial Science and Technology (AIST), 16-1 Onogawa, Tsukuba 305-8569, Japan*

Received December 10, 2001; revised July 4, 2002; accepted July 11, 2002

**The reaction paths of the selective catalytic reduction of $NO_2$ by $C_2H_4$ over H–ferrierite were investigated by identifying and measuring the reactivity of the by-products under various coexisting gas conditions. Nitroethylene (NE), HCN, and HNCO were detected as nitrogen-containing by-products. It was found that there were two reaction pathways for $N_2$ formation: the direct reaction between NE and $NO_2$, and NE decomposition followed by the formation and hydrolysis of HNCO. The latter pathway led to the formation of $NH_3$, which further reacted with $NO_x$ to form $N_2$.** 

*Key Words:* **selective catalytic reduction; H–ferrierite; $NO_2$; product analysis; nitroethylene; HNCO; HCN; hydrolysis; $NH_3$.**

## 1. INTRODUCTION

Ever since Held *et al.* (1) and Iwamoto *et al.* (2) first reported the selective catalytic reduction (SCR) of $NO_x$ with hydrocarbons under excess oxygen, this catalytic process has been recognized as a promising method to remove the $NO_x$ emitted from diesel and lean-burn gasoline engines. However, this method for removing $NO_x$ is so far somewhat impractical, because the $NO_x$ conversion is low and the active temperature range is narrow. To improve this catalytic process, clarification of the reaction mechanism and identification of the key factors for active catalysts are necessary.

In their studies on the reaction mechanism, Hamada *et al.* proposed that the first step of the SCR of $NO_x$ is the oxidation of NO to $NO_2$ (3). It was thought that the subsequent reaction involved the formation and decomposition of intermediates containing a carbon–nitrogen bond. Yokoyama and Misono proposed nitro compounds as intermediates, which were supposed to be formed by the addition of $NO_2$ to a double bond in olefins (4). Cowan *et al.* proposed nitromethane as an intermediate (5), based on the investigation using it as a model intermediate (6, 7). Beutel *et al.* argued that an intermediate containing a carbon–nitrogen bond is produced by the reaction between NO and hydrocarbon without passing through $NO_2$ (8). Obuchi *et al.* investigated the reaction mechanism by using a nitrile oxide compound (–CNO) as a possible intermediate (9). In their studies on elementary reactions involving $N_2$ formation as the final step of the SCR, Ukisu *et al.* (10) and other groups (11, 12) proposed a surface isocyanate as an intermediate on the basis of DRIFT measurements. Radtke *et al.* detected HCN (13) and HNCO (14) in the effluent gases by gas analysis and proposed that the hydrolysis of these compounds results in the formation of $N_2$ (15). However, each of these proposals can only explain part of the whole reaction mechanism.

It is of interest that proton-form zeolites and $Al_2O_3$, which have very poor redox activity, also show the SCR activity (16). The activities of this type of catalyst increase when $NO_2$ is used as a reactant instead of NO. Using this characteristic, various attempts have been made to improve the SCR performance by combining two functionally different catalysts, an NO oxidation catalyst and an active catalyst for the SCR of $NO_2$ (SCR-$NO_2$) (17, 18).

In this study, we attempted to identify the gaseous intermediates and thereby clarify the reaction steps involved in a model SCR-$NO_2$, i.e., selective reduction of $NO_2$ with ethylene, over a proton-form ferrierite (H–ferrierite). The study especially focused on the elucidation of a reaction sequence or network that connects the reactant, $NO_2$, and the desirable product, $N_2$, with feasible gaseous intermediates. Product analysis was carried out for this purpose, with special emphasis on nitrogen-containing compounds, and their reactions under several gaseous environments similar to that of the SCR reaction. H–ferrierite was used as a model catalyst because it has a poor activity with respect to hydrocarbon oxidation but is an active catalyst for SCR with olefins (19). This enables reducing the complexities in the reaction steps arising from the various oxidation paths. Ethylene was used as a reductant because it is structurally

[1] To whom correspondence should be addressed. Fax: +81-298-61-8259. E-mail: tty-namba@aist.go.jp.



0021-9517/02 $35.00

the simplest olefin. By investigating this simplified SCR reaction system, we attempted to clarify its nitrogen chemistry and essential steps of the SCR-$NO_2$.

## 2. EXPERIMENTAL

### 2.1. Catalyst Preparation

Two kinds of H–ferrierites (abbreviated H–FER-17 and H–FER-64) and Na–ferrierite were used as catalysts. H–FER-17 was commercially provided by M/s Tosoh, Japan (HSZ-720HOA, $SiO_2/Al_2O_3 = 17.0$, BET surface area = 302 $m^2/g$). H–FER-64 was obtained by calcination of $NH_4$-form ferrierite (Tosoh, $NH_4$–ferrierite, $SiO_2/Al_2O_3 = 64.0$, BET surface area = 356 $m^2/g$) at 500°C for 1 h. Na–ferrierite was obtained by ion exchange of H–FER-17 in 0.035 mol/L NaOH at 80°C for 24 h. These catalysts were pelletized to obtain particles with their size in the range of 250–600 $\mu$m.

A honeycomb catalyst loaded with ca. 50 mg of the wash-coated H–FER-17 layer was prepared for the mechanistic study on this catalyst. H–FER-17, silica binder (Catalysis & Chemicals IND. Co., Cataloid S-20L, containing 20 wt% $SiO_2$), and water were mixed in a ball mill at a weight ratio of 1 : 2 : 3 and made into slurry. A cylindrical piece of honeycomb (8-mm $\phi \times$ 9-mm $L$) was cut out from a cordierite honeycomb (NGK Insulator, Honeyceram, 400 cells/in.$^2$), wash-coated with the above slurry, dried at 110°C for 30 min, and calcined at 500°C for 1 h.

### 2.2. Characterization

X-ray diffraction analysis (Rigaku, RINT2000) was used for confirming that the Na–ferrierite maintained the ferrierite structure after ion exchange.

Temperature-programmed desorption of $NH_3$ ($NH_3$-TPD) was carried out on a TPD apparatus (Bel Japan Inc., TPD-1-AT), which is equipped with a mass spectrometer for the detection of desorbed $NH_3$. About 50 mg of sample was pretreated in 50 ml/min of He flow at 500°C for 1 h. It was then cooled and exposed to $NH_3$ at 100°C for 1 h under an equilibrium pressure of 20 Torr. After evacuation at the same temperature for 1 h, the TPD measurement was taken from 100 to 600°C in the 50 ml/min He flow with a heating rate of 10°C/min.

### 2.3. Catalytic Activity Test

*2.3.1. Selective catalytic reduction of $NO_2$ by $C_2H_4$ ($C_2H_4$-SCR-$NO_2$).* Pelletized catalysts (50 mg) and the honeycomb catalyst were installed in a quartz tube (8-mm internal diameter) and were pretreated in a 5% $O_2$/He flow at 500°C for 1 h. The effect of reaction temperature on the catalytic reaction was measured in a 160 ml/min flow of feed gas (1000 ppm $NO_2$, 1050 ppm $C_2H_4$, and 5% $O_2$ in He) at temperatures from 500 to 200°C in steps of 25°C. Under these conditions, the space velocity specific to the apparent volume of the honeycomb catalyst was 21,000 $h^{-1}$. Analysis of the effluent gas was carried out by gas chromatography and FT-IR spectrometry. The gas chromatograph (Agilent, MicroGC) was equipped with an MS-5A PROT column (for $N_2$ and CO analysis) and a PolaPROT Q column (for $CO_2$ and $N_2O$ analysis). An FT-IR spectrometer (Nicolet, Magna 560), which was equipped with a multireflection gas cell (Gemini Specialty Optics, Mercury Series, optical path length = 2 m) and a MCT detector, was used for the analysis of gaseous NO, $NO_2$, $C_2H_4$, and other by-products (18). The FT-IR measurements were performed at a resolution of 0.5 $cm^{-1}$ and a spectrum was obtained by integrating 50 scans, which took ca. 80 s. The concentrations of each component were estimated from the intensity of the IR absorption peak specific to each component. The integrated peak range in the FT-IR gas analysis and the accuracy of both the GC and the FT-IR analyses are listed in Table 1.

**TABLE 1**

**Accuracy of Product Analysis**

| Compound | Method | Integrated peak range in IR analysis ($cm^{-1}$) | Range (ppm) | Error (ppm) |
|---|---|---|---|---|
| NO | IR | 1911.4–1913.4 | 0–1100 | ±10 |
| $NO_2$ | IR | 1643.2–1644.4 | 0–1100 | ±20 |
| $N_2$ | GC | — | 0–200 | ±3 |
| $N_2O$ | GC | — | 0–200 | ±3 |
| $NH_3$ | IR | 1121.5–1122.6 | 0–300 | ±5 |
| CO | GC | — | 0–600 | ±3 |
| $CO_2$ | GC | — | 0–3000 | ±3 |
| $C_2H_4$ | IR | 948.2–950.5 | 0–1000 | ±20 |
| HCHO | IR | 2813.2–2815.6 | 0–250 | ±10 |
| HCN | IR | 711.5–715.8 | 0–300 | ±6 |
| HNCO | IR | 2257.5–2258.6 | 0–150 | ±6 |
| NE | IR | 1545.9–1547.2 | 0–300 | ±4 |

The dependence of by-product formation on contact time for $C_2H_4$-SCR-$NO_2$ was investigated at 250, 350, and 450°C under the same gas composition as was used for the temperature dependency measurement. The gas flow rate was varied from 60 to 300 ml/min, which corresponds to 0.09–0.45 s of contact time, or a space velocity of 8,000–40,000 $h^{-1}$.

*2.3.2. Reaction of by-products.* The effect of coexisting gas on the reaction of the by-products found in $C_2H_4$-SCR-$NO_2$ and $NH_3$, one of their derivatives, was investigated using the honeycomb catalyst. All tests were performed in the same tubular flow reactor as was used for the $C_2H_4$-SCR-$NO_2$ and the flow rates were set at 160 ml/min.

Nitroethylene ($C_2H_3NO_2$; NE) was synthesized according to the literature (20). Reactant gases containing ca. 200 ppm NE were obtained by passing a predetermined flow rate of He through NE liquid maintained at 0°C. Isocyanic acid (HNCO) was generated by controlled thermal decomposition of cyanuric acid (Wako Pure Chemicals). Reactant gases containing 30–110 ppm HNCO and 500 ppm

$H_2O$ were obtained by passing a metered flow of He carrier through the HNCO generator and liquid $H_2O$ at 0°C. Hydrogen cyanide (HCN) was produced continuously by introducing a metered flow of a 0.1 M NaOH (Wako Pure Chemicals) solution containing 1.4% KCN (Wako Pure Chemicals) into 1 M $H_2SO_4$ (Wako Pure Chemicals) at 0°C. Reactant gases containing 220–300 ppm HCN and ca. 2000 ppm $H_2O$ were obtained by passing a metered flow of He carrier through the above $H_2SO_4$ solution. The reactions of these nitrogen-containing compounds were performed under four different gas conditions: in inert gas (He), in 5% $O_2$, in 5% $O_2 + 1000$ ppm NO, and in 5% $O_2 + 1000$ ppm $NO_2$, at temperatures ranging from 500 to 150°C in steps of 50°C.

Selective catalytic reductions of NO and $NO_2$ with $NH_3$ ($NH_3$-SCR) were performed by using reactant gases containing 360 ppm $NH_3 + 1000$ ppm $NO + 5\%$ $O_2$ and 400 ppm $NH_3 + 1000$ ppm $NO_2 + 5\%$ $O_2$. Measurements were carried out at temperatures ranging from 500 to 150°C in steps of 50°C.

Because of the uncontrollable drift in the inlet concentration of the nitrogen-containing compounds, the results of their reactions were expressed in most cases in terms of the specific consumption (SC) and specific production (SP), which were defined as follows:

$$\mathrm{SC}(\%) = \frac{\text{Object inlet conc.} - \text{Object outlet conc. (ppm)}}{\text{Inlet conc. of reactant of interest (ppm)}} \times 100;$$

$$\mathrm{SP}(\%) = \frac{\text{Product conc. (ppm)}}{\text{Inlet conc. of reactant of interest (ppm)}} \times 100.$$

The specific consumption of the reactant of interest is equivalent to its conversion as used conventionally.

## 3. RESULTS

### 3.1. Overall $C_2H_4$-SCR-$NO_2$ and Its By-products

Figure 1 shows the $C_2H_4$-SCR-$NO_2$ activity for the three kinds of pelletized ferrierite catalysts. $NO_x$ conversion over H–FER-17 reached a level of 50–60% above 225°C, while that over H–FER-64 was substantially lower, increasing with temperature but reaching only to ca. 40%, even at the highest temperature investigated. Furthermore, Na–ferrierite showed a maximum $NO_x$ conversion of only 18% at 250°C.

The amount of desorbed $NH_3$ for the above three catalysts in the TPD measurement, which corresponds to the number of acid sites, is listed in Table 2. H–FER-17 showed the highest total amount of desorbed $NH_3$, and the amount decreased with an increase in the $SiO_2/Al_2O_3$ ratio and with ion exchange of proton with Na. Na–ferrierite had no peak at higher temperatures. Although the total amount of desorbed $NH_3$ over Na–ferrierite was higher than that over H–FER-64, the $C_2H_4$-SCR-$NO_2$ activity of Na–ferrierite was lower than that of H–FER-64, especially above 250°C. These results suggest that the activity correlates with the number of acid sites and particularly that of strong acid sites, most probably proton sites, corresponding to the higher temperature peak of $NH_3$ desorption.

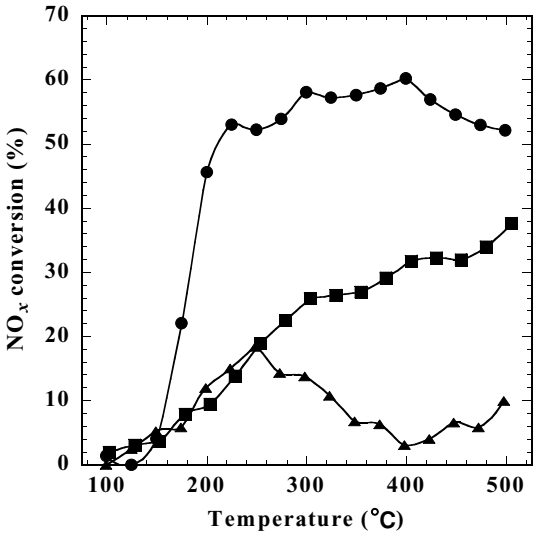


**FIG. 1.** Catalytic activity for $C_2H_4$-SCR-$NO_2$ over H–FER-17 (●), H–FER-64 (■), and Na–ferrierite (▲). Feed gas was composed of 1000 ppm $NO_2$, 1050 ppm $C_2H_4$, and 5% $O_2$.

Since H–FER-17 showed the highest activity, we focused on the elucidation of reaction pathways over this type of catalyst in a honeycomb form.

Figure 2a shows the temperature dependence of $C_2H_4$-SCR-$NO_2$. The $NO_x$ was partly consumed and $N_2$ was formed, even at temperatures as low as 200°C. The consumption of $NO_x$ increased with increasing temperature up to 250°C and then reached an almost constant level of ca. 450 ppm. The $N_2$ concentration increased up to 375°C and then attained an almost constant level of ca. 160 ppm. The consumption of $C_2H_4$ was nearly constant at 270 ppm between 225 and 375°C but increased above 375°C. The $CO_2$ and CO concentrations were close to each other below 300°C, but above 300°C the $CO_2$ concentration decreased with increasing temperature, while the CO concentration

**TABLE 2**

**Amount of $NH_3$ Desorption by TPD**

| Sample | Desorbed amount (mmol/g) | | |
|---|---|---|---|
| | Low peak (°C[a]) | High peak (°C[a]) | Total |
| H–FER-17 | 0.31 (174) | 0.56 (427) | 0.87 |
| H–FER-64 | 0.06 (167) | 0.18 (372) | 0.24 |
| Na–ferrierite | 0.60 (220) | — | 0.60 |

[a] The temperature of $NH_3$ desorption peak.

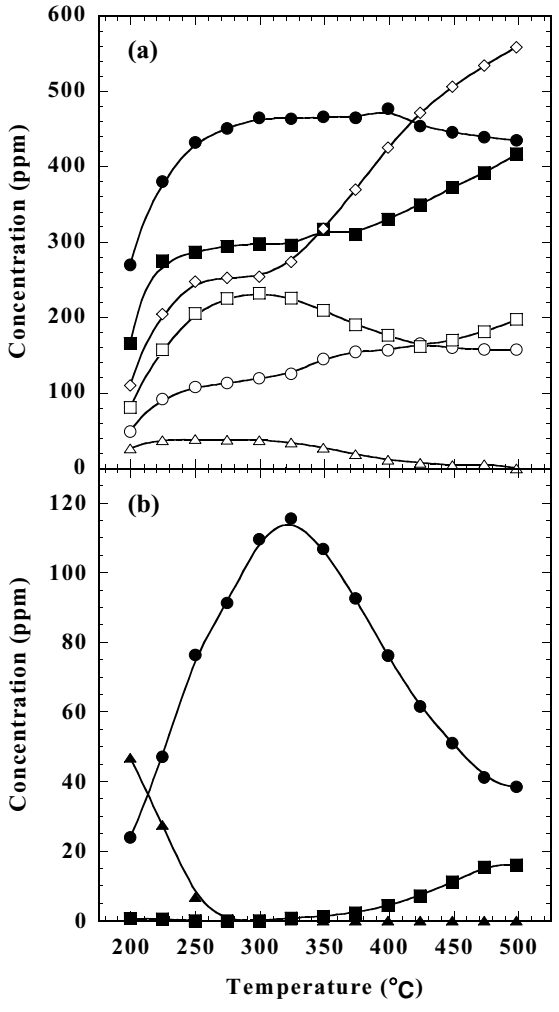


**FIG. 2.** Catalytic activity for $C_2H_4$-SCR-$NO_2$ over a honeycomb-type catalyst. Feed gas was composed of 1000 ppm $NO_2$, 1050 ppm $C_2H_4$, and 5% $O_2$. (a) Symbols indicate consumption of $NO_x$ (●) and $C_2H_4$ (■) and production of $N_2$ (○), $N_2O$ (△), CO (◇), and $CO_2$ (□). (b) Symbols indicate production of HCN (●), HNCO (■), and NE (▲).

increased with increasing temperature. $N_2O$ was formed below 400°C.

NE, HNCO, and HCN were detected as nitrogen-containing by-products in this reaction (Fig. 2b). NE was only detected below 275°C. HNCO was observed above 350°C, and its concentration increased with increasing temperature. HCN was found over the whole temperature range investigated, and the maximum production of 116 ppm was obtained at 325°C.

To check whether the observed by-products are inactive species that do not undergo further conversion or are active intermediates toward $N_2$ formation, the dependence of the by-product concentration on contact time was investigated at 250, 350, and 450°C (Fig. 3). NE appeared only at shorter contact times at 250°C. The ratio of $N_2$ to NE significantly decreased with decreasing contact time and was extrapolated to zero at zero contact time. HNCO production was very low for all the contact times investigated. At 250°C, the HCN concentration increased with increasing contact time and reached a constant level at 0.15 s, but at 350 and 450°C it decreased constantly with increasing contact time. Also, at 250°C, the ratio of $N_2$ to HCN only decreased slightly with decreasing contact time and was not extrapolated to zero at zero contact time. At 350 and 450°C, on the other hand, the ratio was extrapolated to almost zero at zero contact time. These results show that NE is clearly an intermediate and HCN above 350°C is likely to be an intermediate of $C_2H_4$-SCR-$NO_2$. The possibility of HNCO being an intermediate was not determined from this experiment and this was therefore investigated by the following reactivity measurements.

### *3.2. Reactions of By-products*

*3.2.1. Nitroethylene.* Figure 4 shows the results of the NE reaction under various coexisting gas conditions.

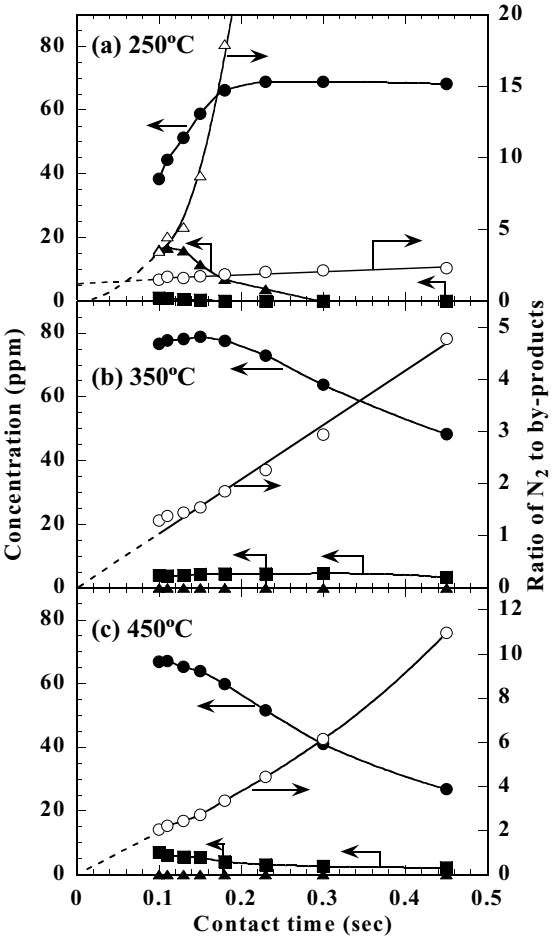


**FIG. 3.** Dependence of by-product concentration on contact time for $C_2H_4$-SCR-$NO_2$. Feed gas was composed of 1050 ppm $NO_2$, 1040 ppm $C_2H_4$, and 5% $O_2$. Symbols indicate concentration of HCN (●), HNCO (■), and NE (▲) and the ratio of $N_2$ to HCN (○) and NE (△).

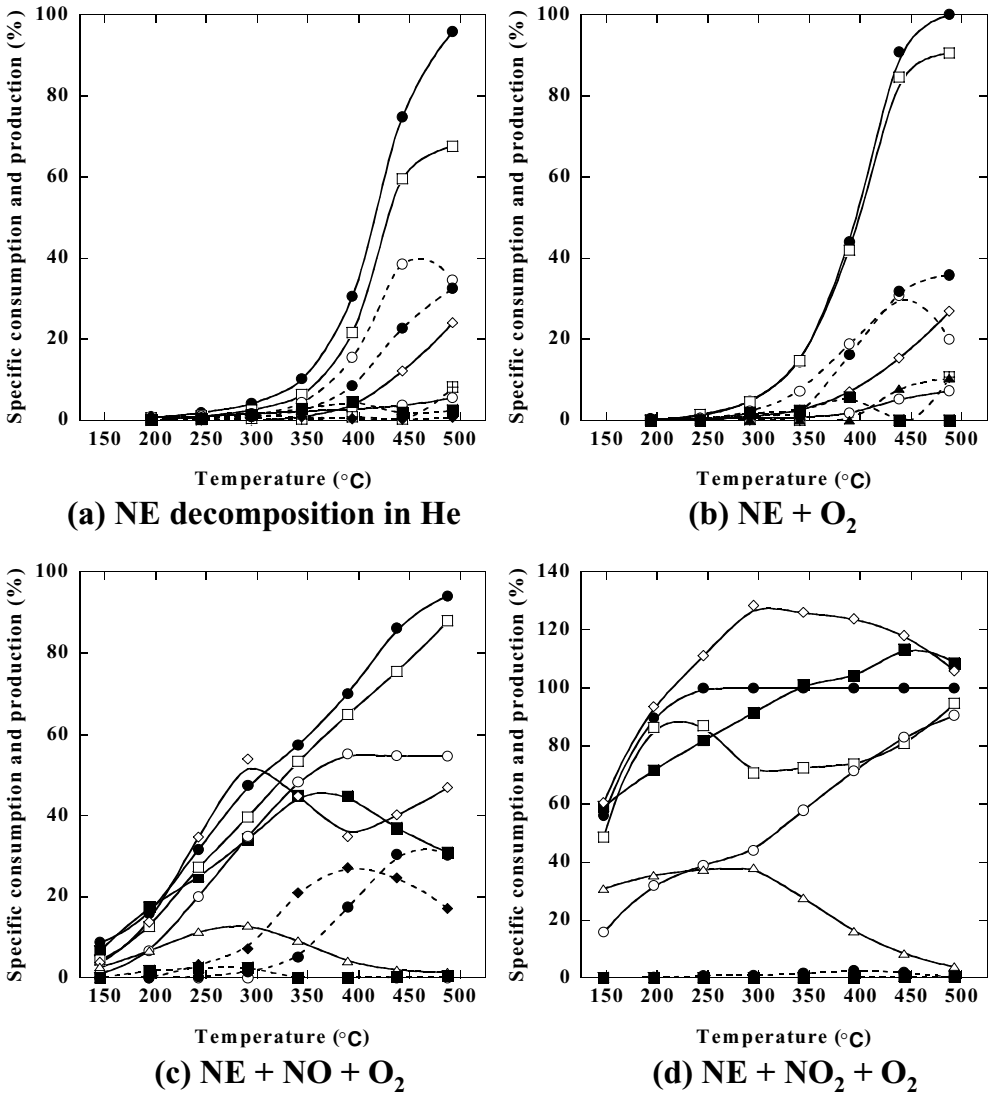


**FIG. 4.** Decomposition activity of NE under various coexisting gas conditions. Results are expressed in SC and SP (%). The reactant of interest was NE. Concentrations of reactants were 170–230 ppm NE, 5% $O_2$, 1000 ppm NO, and 1070 ppm $NO_2$. Symbols indicate SC of NE (—●—) and $NO_x$ (—■—) and SP of $N_2$ (—○—), $N_2O$ (—△—), $CO_2$ (—□—), CO (—◇—), $NH_3$ (---○---), HCN (---●---), HNCO (---■---), HCHO (---◆---), $C_2H_4$ (---▲---), and $NO_x$ (---⊞---).

NE decomposed above 250°C in He (Fig. 4a). The main products were $CO_2$, $NH_3$, HCN, and CO. Other minor products were NO, $NO_2$, HNCO, HCHO, and $C_2H_4$. The results in the presence of $O_2$ (Fig. 4b) were almost the same as those in He. These results indicate that the self-decomposition of NE proceeds more easily than its reaction with $O_2$. It is noted that under these gaseous conditions, $CO_2$ production was roughly equal to NE consumption.

In the presence of NO + $O_2$, NE consumption at low temperatures increased remarkably compared with that in the absence of NO (Fig. 4c). The ratios of $NO_x$ consumption and the production of $N_2$, $CO_2$, and CO to NE consumption were roughly unity below 350°C. In other words, one $N_2$ molecule, one $CO_2$ molecule, and one CO molecule were apparently produced from one NE molecule and one NO molecule. $N_2O$, HCHO, HCN, and a trace of HNCO were observed as minor products, but no $NH_3$ was detected.

The reaction of NE in the presence of $NO_2 + O_2$ was significantly different from that under the other three sets of conditions (Fig. 4d). NE was completely converted above 225°C, a large amount of $N_2O$ was formed below 300°C, and $N_2$ was the dominant product above 300°C. It is obvious from this result that NE was able to produce $N_2$ or $N_2O$ quite effectively even at temperatures as low as 150°C in the presence of $NO_2$. The ratios of the $N_2 + N_2O$ production and $NO_x$ consumption to the NE consumption were roughly unity. Also, CO production and $CO_2$ production were almost equal to the NE consumption below 200°C but

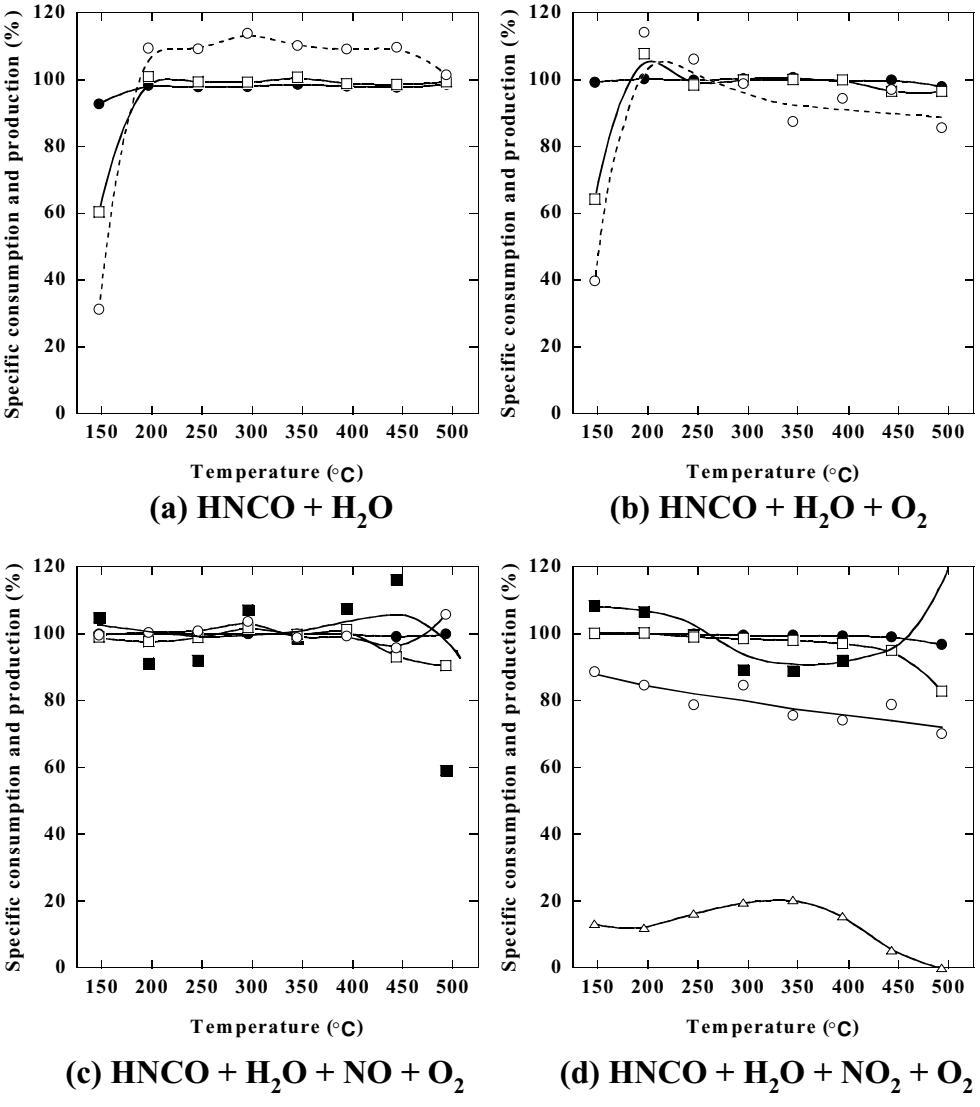


**FIG. 5.** Decomposition activity of HNCO under various coexisting gas conditions. The reactant of interest was HNCO. Concentrations of reactants were 30–110 ppm HNCO, 500 ppm $H_2O$, 5% $O_2$, 1000 ppm NO, and 1000 ppm $NO_2$. Symbols indicate SC of HNCO (—●—) and $NO_x$ (—■—) and SP of $N_2$ (—○—), $N_2O$ (—△—), $CO_2$ (—□—), and $NH_3$ (---○---).

varied in opposite directions above 200°C. Only traces of HCN and HNCO were detected. The promotion of NE consumption in the presence of NO or $NO_2$ and the quantitative relationship between NE consumption and the product concentrations strongly suggest that NE is an intermediate for $N_2$ and $N_2O$ formation in $C_2H_4$-SCR-$NO_2$, and reacts with NO or $NO_2$ in a ratio of 1 : 1.

*3.2.2. HNCO.* Figure 5 shows the results of the HNCO reaction in the presence 500 ppm $H_2O$ and other coexisting gases.

Above 200°C, HNCO was completely converted into equal amounts of $CO_2$ and $NH_3$ in the presence of only $H_2O$ vapor (Fig. 5a). It is evident that the following hydrolysis occurred preferentially:

$$HNCO + H_2O \rightarrow NH_3 + CO_2.$$

The same reaction occurred in the presence of $O_2$ (Fig. 5b). In the presence of $NO + O_2$, the reactivity of HNCO became higher still, with complete conversion being achieved even below 200°C (Fig. 5c). Since the amount of $CO_2$ produced was nearly equal to the amount of HNCO consumed, hydrolysis was also suggested to predominate under these conditions. In addition, because the HNCO and $NO_x$ consumptions were almost equal to each other and because an amount of $N_2$ equivalent to these values was formed without forming $NH_3$, this indicates that the $NH_3$ formed by HNCO hydrolysis reacted with NO to form $N_2$, according

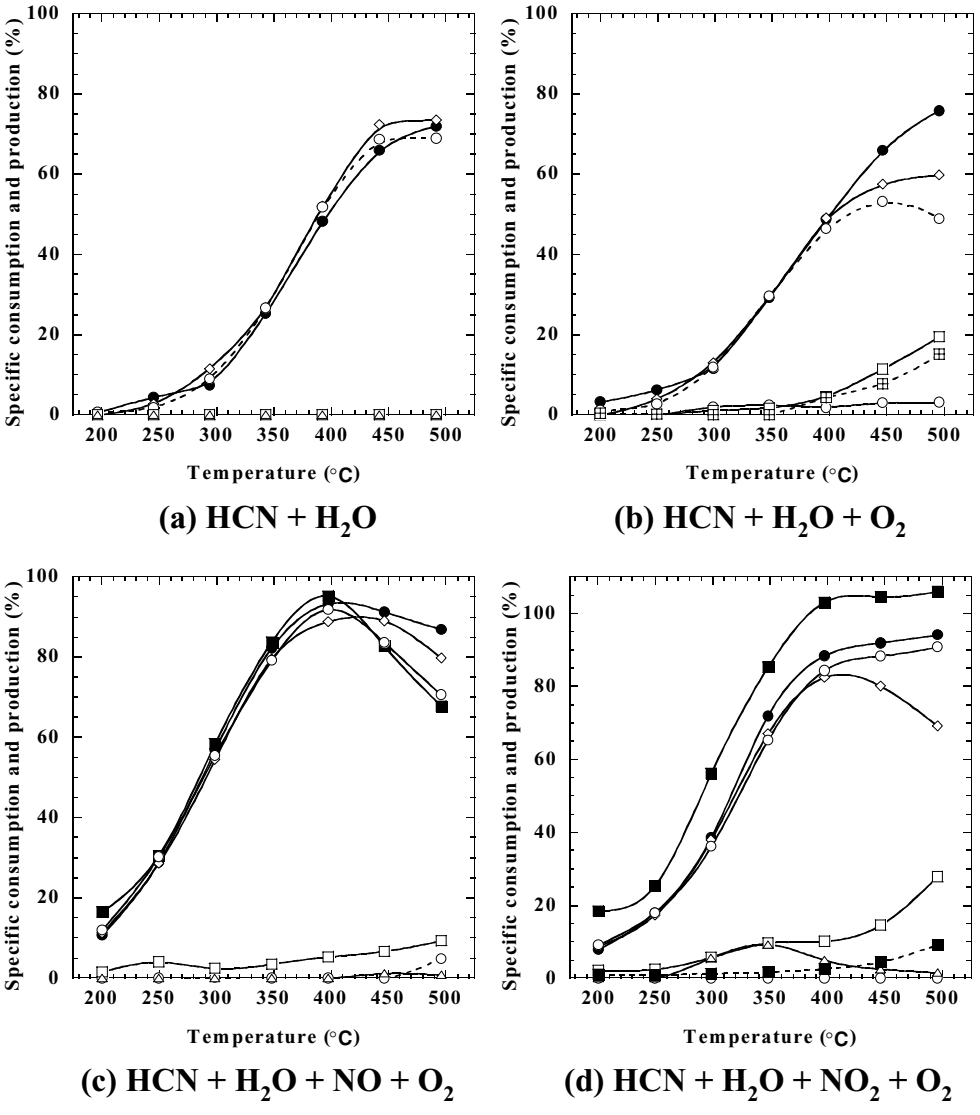


**FIG. 6.** Decomposition activity of HCN under various coexisting gas conditions. The reactant of interest was HCN. Concentrations of reactants were 220–300 ppm HCN, 2000 ppm $H_2O$, 5% $O_2$, 1000 ppm NO, and 1000 ppm $NO_2$. Symbols indicate SC of HCN (—●—) and $NO_x$ (—■—) and SP of $N_2$ (—○—), $N_2O$ (—△—), $CO_2$ (—□—), CO (—◇—), $NH_3$ (---○---), HNCO (---■---), and $NO_x$ (---⊞---).

to the conventional $NH_3$-SCR:

$$NH_3 + NO + \frac{1}{4}O_2 \rightarrow N_2 + H_2O.$$

In the presence of $NO_2 + O_2$ (Fig. 5d), HNCO was also completely converted below 200°C and amounts of $N_2 + N_2O$ and $CO_2$ equivalent to the amount of HNCO consumed were formed. Again, the amount of $CO_2$ formation is almost equal to the HNCO consumption, the absence of $NH_3$ suggests that the HNCO was predominantly hydrolyzed into $CO_2$ and $NH_3$, and $NH_3$ reacted further with $NO_2$ to form $N_2$ and partly $N_2O$ in this case.

*3.2.3. HCN.* Figure 6 shows the results of the HCN reaction in the presence of 2000 ppm $H_2O$ and other coexisting gases.

With only $H_2O$ vapor, the HCN reaction proceeded above 200°C. Almost equivalent quantities of CO and $NH_3$ were produced with respect to observed HCN consumption at all temperatures. This suggests that the following hydrolysis reaction occurred exclusively:

$$HCN + H_2O \rightarrow NH_3 + CO.$$

In the presence of $O_2$, hydrolysis seemed to still be the dominant reaction below 400°C, producing amounts of $NH_3$ and CO almost equivalent to that of HCN consumption (Fig. 6b). NO and $CO_2$ were observed above 400°C. In the presence of $NO + O_2$, HCN consumption increased compared to that in the absence of NO at all temperatures (Fig. 6c). $NO_x$ consumption was almost equal to HCN consumption, simultaneously producing equivalent amounts

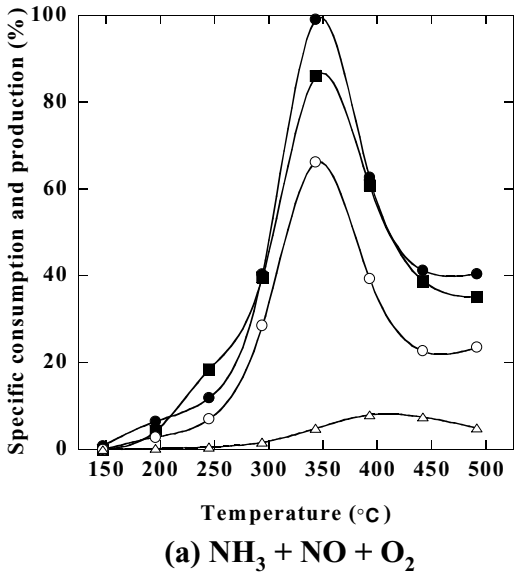


**FIG. 7.** Conventional $NH_3$-SCR activity. (a, b) Results for the $NH_3 + NO + O_2$ and $NH_3 + NO_2 + O_2$ reactions, respectively. The reactant of interest was $NH_3$. Feed gas was composed of 360–400 ppm $NH_3$, 1000 ppm NO or $NO_2$, and 5% $O_2$. Symbols indicate SC of $NH_3$ (●) and $NO_x$ (■) and SP of $N_2$ (○) and $N_2O$ (△).

of $N_2$ and CO. This suggests that in this case HCN was also dominantly decomposed by hydrolysis. The absence of $NH_3$, except for a trace at 500°C, suggests that conventional $NH_3$-SCR proceeded after the HCN hydrolysis in a way similar to the HNCO reaction. In the presence of $NO_2 + O_2$, the reaction profiles were similar to those in the presence of $NO + O_2$ (Fig. 6d), suggesting that the HCN hydrolysis followed by the $NH_3 + NO_2$ reaction proceeded. A small amount of HNCO was formed. HONO was detected but not quantified in the FT-IR gas analysis.

*3.2.4. Selective reduction of $NO_x$ by $NH_3$.* Although no $NH_3$ was detected during the $C_2H_4$-SCR-$NO_2$, it was formed by the decomposition of NE, HCN, and HNCO, and there were strong suggestions that it reacted with $NO_x$. Accordingly, the $NH_3$-SCR was investigated over the same catalyst, as shown in Fig. 7. In the case of $NH_3$-SCR with NO, the $NH_3$ and $NO_x$ consumption had a maximum at 350°C (Fig. 7a). $N_2$ was the dominant product, and a small amount of $N_2O$ was formed at high temperatures. In $NH_3$-SCR with $NO_2$, the $NH_3$ was completely converted at all of the temperatures investigated (Fig. 7b). $N_2$ was the major product, but an appreciable quantity of $N_2O$ was also formed, with a maximum at ca. 250°C. Nitrogen-material balance was not obtained at 150–200°C, which indicates that certain nitrogen-containing compounds with low volatility and which are undetectable by FT-IR gas analysis, such as $HNO_3$ and $NH_4NO_3$, were produced at this temperature.

## 4. DISCUSSION

### *4.1. Nitroethylene as a Direct Precursor of $N_2$ and $N_2O$*

NE is a gaseous nitro compound, which we have found as a by-product for the first time in the SCR of $NO_x$ with hydrocarbons (21). On the basis of the results obtained in this study, the role of NE in the reaction pathways of $C_2H_4$-SCR-$NO_2$ is discussed below.

The results shown in Fig. 3 suggest that NE was an intermediate of the SCR reaction at 250°C. Furthermore, it is obvious from Fig. 4d that the $NE + NO_2 + O_2$ system produces $N_2$ and $N_2O$ very rapidly. The high reactivity of NE with $NO_2$ above 150°C and the complete conversion of NE above 250°C are in agreement with the results of the $C_2H_4$-SCR-$NO_2$, in which remarkable amounts of $N_2$ and $N_2O$ are formed around 200°C and the NE observed at lower temperatures is missing above 275°C (Fig. 2). These results strongly suggest that a direct reaction between NE and $NO_2$ takes place in the $C_2H_4$-SCR-$NO_2$. However, we could not further confirm this most promising pathway experimentally, since there were no outstanding by-products in the $NE + NO_2 + O_2$ reaction, and no literature was found concerning theoretical calculations on the reaction of NE with $NO_2$.

### *4.2. Nitroethylene as a Precursor of HNCO and HCN*

In contrast to the reaction in the presence of $NO_2$, the reaction of NE in He and in the presence of $O_2$ and $NO + O_2$ resulted in the formation of common minor products, such as HNCO, HCN, and HCHO (Figs. 4a–4c). Furthermore, $CO_2$ was formed at a concentration almost equivalent to that of NE consumption in these cases. Thus, it is speculated that NE decomposes in a similar manner under these conditions. The production of the above minor products by the thermal decomposition of NE was theoretically predicted

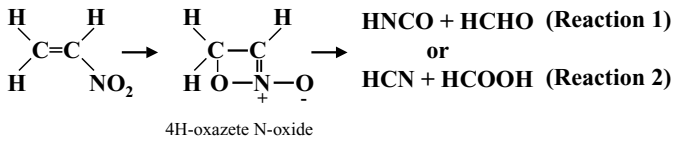


**SCHEME 1.** Thermal decomposition of NE.

by Shamov and Khrapkovskii (22), as shown in Scheme 1: NE decomposes through a four-membered-ring compound (4*H*-oxazete *N*-oxide) into HNCO + HCHO (Reaction 1) or HCN + HCOOH (Reaction 2). Taking into account our supplementary experimental results on the decomposition of HCHO and HCOOH over H–ferrierite, out of these four possible products of NE decomposition, only HNCO can produce $CO_2$ through its hydrolysis in the absence of $NO_2$. Therefore, the observation of a rate of $CO_2$ formation almost equivalent to NE consumption suggested to us that the decomposition of NE in the form of Reaction 1 is likely to be the main route followed under these reaction conditions.

Although HCN was confirmed as being formed from NE, the HCN concentrations in the $C_2H_4$-SCR-$NO_2$ (Fig. 2) were much higher than those expected by this pathway. For example, at 350°C, the specific production of HCN in the NE reaction was estimated from Figs. 4a–4c to be at most 5%, which would necessitate formation of 2140 ppm NE for the 107 ppm HCN actually observed in the $C_2H_4$-SCR-$NO_2$ at this temperature. This result clearly demonstrates that there are other reaction pathways for producing HCN, but we have no experimental results to identify these pathways as yet. One possible pathway is the formation and decomposition of nitrosoethylene, which is predicted to decompose into HCN and HCHO through a four-membered-ring structure, similar to NE decomposition (23).

### 4.3. *HNCO and HCN as a Precursor of $NH_3$*

The hydrolysis of HNCO to $NH_3$ and $CO_2$ proceeded very easily over the whole temperature range investigated for the $C_2H_4$-SCR-$NO_2$, independent of the coexisting gases (Fig. 5). HNCO is known to hydrolyze rapidly on an $Al_2O_3$ catalyst even at room temperature (24). This high reactivity for hydrolysis suggests that HNCO is an intermediate of this SCR pathway. The extremely low HNCO concentrations in $C_2H_4$-SCR-$NO_2$ (Fig. 2) regardless of contact time (Fig. 3) and in the NE reactions (Fig. 4) are attributable to its high reactivity.

The results of dependence on contact time (Fig. 3) suggested that HCN was also an intermediate for $N_2$ formation above 350°C. The formation of HCN as a by-product and its role as a possible intermediate to the formation of $N_2$ over $Al_2O_3$ (13) and $Cu/Al_2O_3$ (15) in SCR has also been reported. Figure 6 indicates that the HCN conversion was enhanced by the presence of $NO_x$. This enhancement is attributed to the elimination of adsorbed $NH_3$ on the proton sites of the H–ferrierite, which are most probably the active sites for hydrolysis, by the reaction with $NO_x$. There have been several studies concerning the obstruction of catalytic reactions by $NH_3$ adsorbed on acid sites (25–27).

In the presence of $NO_2$, the HCN seemed to be oxidized to HNCO, probably due to the strong oxidation ability of $NO_2$ (Fig. 6d). Taking the high reactivity of HNCO for hydrolysis into account, part of the HCN is supposed to be converted to $NH_3$ through its oxidation to HNCO under this gaseous condition.

### 4.4. *$N_2$ and $N_2O$ Formation through $NH_3$*

$NH_3$, which was formed by HNCO and HCN hydrolysis, reacted with $NO_2$ very rapidly and also reacted with NO at an appreciable rate at around 350°C to form $N_2$ and $N_2O$ in the presence of $O_2$ over H–ferrierite (Fig. 7). Appreciable quantities of $N_2O$ were formed when $NO_2$ was present in the reactant (Figs. 5–7). This is in agreement with our previous result, which showed that the $NO_2/NO_x$ ratio affects the selectivity to $N_2$ and $N_2O$ in $NH_3$-SCR on the same catalyst (28). Possible pathways for $N_2$ and $N_2O$ formation from $NH_3$ are as follows (29–32):

$$\begin{aligned} NO_2 + NO + H_2O &\rightarrow 2HONO, \\ 2NO_2 + H_2O &\rightarrow HONO + HNO_3, \\ NH_3 + HONO &\rightarrow NH_4NO_2 \rightarrow N_2 + H_2O, \\ NH_3 + HNO_3 &\rightarrow NH_4NO_3 \rightarrow N_2O + H_2O. \end{aligned}$$

### 4.5. *Total Reaction Pathways of $C_2H_4$-SCR-$NO_2$*

Based on the above discussion for the reaction of each nitrogen-containing compound, the reaction network of $C_2H_4$-SCR-$NO_2$ was estimated, as shown schematically in Fig. 8. The reaction sequence starts with the addition of $NO_2$ molecules to $C_2H_4$, which leads to NE formation. In the presence of excess $NO_2$, the NE reacts directly with $NO_2$ to form $N_2$ and $N_2O$. Under $NO_2$-deficient conditions, the NE mainly decomposes into HNCO, which is easily further hydrolyzed into $NH_3$ and $CO_2$. HCN may be partly produced by the decomposition of NE, but it is produced mostly through other unidentified pathways. HCN is a relatively stable by-product at low temperature, but it is also supposed to be involved as an intermediate at high temperature, since it is hydrolyzed into $NH_3$ and CO or converted to the more reactive HNCO in the presence of $NO_2$. Finally, the $NH_3$ formed from HNCO and HCN reacts with $NO_2$ and NO to form $N_2$ and $N_2O$.

The overall $C_2H_4$-SCR-$NO_2$ is a redox reaction between $C_2H_4$ and $NO_2$, but it should be noted that the valence of the N atoms in the above reaction network does not monotonically approach the neutral state (in $N_2$) from the reactant $NO_2$. The N atom in NE, which is in an oxidative state, is

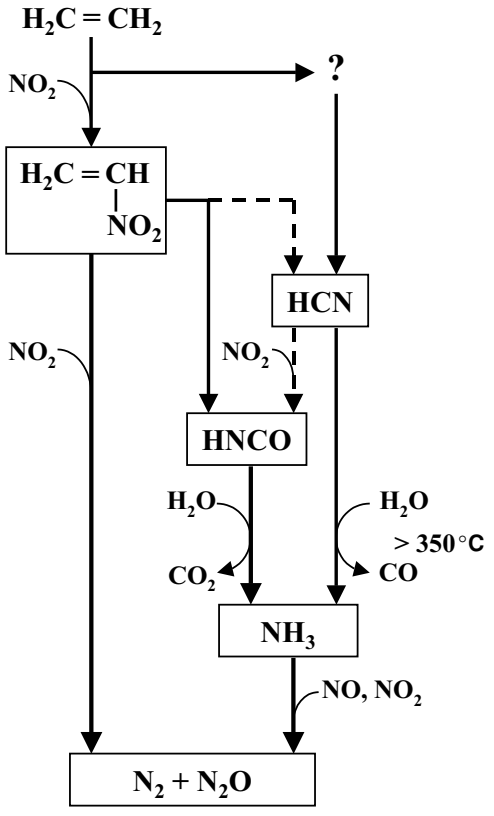


**FIG. 8.** Speculated mechanism for selective catalytic reduction of $NO_x$ by $C_2H_4$ over H–ferrierite.

temporarily changed to an excessively reduced state if the NE is decomposed into HNCO and then is converted to $NH_3$. $N_2$ is formed from these species by the combination with oxidative $NO_2$ and NO. We think that a step in which a nitro compound is formed, or, in other words, a step in which a C–N bond is formed, is essential in these SCR processes, because after the establishment of this bond, the N atom involved seems to be readily converted to excessively reduced states and then to $N_2$.

In this study we have focused our attention on understanding the nitrogen chemistry of a model SCR reaction and the elucidation of promising pathways connecting the reactants to the products through gaseous intermediates. It is difficult to clearly distinguish an intermediate from an inactive by-product. However, we suppose that if a by-product has a reactivity comparable to the rate of the main reaction and is converted to the same products under similar conditions, it is regarded as an intermediate. The key intermediates may also be in the adsorbed phase. To elucidate the integrated mechanism, it would be necessary to further identify the adsorbed intermediates and to clarify their relationship with gaseous species. Some of the characteristics of the catalyst, e.g., strength and density of the acid sites, may bear a relationship with the rate of each elementary reaction step. However, this clarification is beyond the scope of the present study. Further work adopting *in situ* studies will throw more light on this aspect.

## 5. CONCLUSIONS

The reaction paths for the selective reduction of $NO_2$ with $C_2H_4$ ($C_2H_4$-SCR-$NO_2$) over H–ferrierite were studied by investigating the formation and reaction of the by-products. The results are summarized as follows:

1. Nitroethylene (NE), HNCO, and HCN were detected as nitrogen-containing by-products in $C_2H_4$-SCR-$NO_2$.
2. NE was converted to HNCO, HCN, $NH_3$, HCHO, CO, and $CO_2$ in the absence of $NO_x$. In the presence of $NO_2$, the NE may directly react with $NO_2$ to form $N_2$ and $N_2O$.
3. HNCO had a high reactivity for hydrolysis and is completely decomposed into $NH_3$ and $CO_2$ above 200°C. HNCO hydrolysis followed by the reaction of $NH_3$ with $NO_x$ to form $N_2$ is a very feasible pathway.
4. HCN was mostly hydrolyzed to $NH_3$ and CO at high temperatures and partly oxidized to HNCO in the presence of $NO_2$. The main pathway for HCN formation in the SCR is still unknown, since the HCN concentrations were much higher than the value predicted by the decomposition of NE.
5. $N_2$ and $N_2O$ were formed by the reactions of $NH_3$ with NO, and $NH_3$ with $NO_2$, the latter reaction being much faster.
6. A reaction network was proposed for $C_2H_4$-SCR-$NO_2$, in which $NO_2$ is converted to $N_2$ and $N_2O$, through the formation of NE followed by its reaction with $NO_2$ or its decomposition into mainly HNCO, subsequent hydrolysis to $NH_3$, and finally its reaction with $NO_x$.

## REFERENCES

1. Held, W., König, A., Richter, T., and Puppe, L., "Catalytic $HO_x$ Reduction in Net Oxidizing Exhaust Gas," SAE Tech. Pap. Ser. No. 900496 (1990).
2. Iwamoto, M., Yahiro, H., Shundo, S., Yu-u, Y., and Mizuno, N., *Appl. Catal.* **69**, L15 (1991).
3. Hamada, H., Kintaichi, Y., Sasaki, M., and Ito, T., *Appl. Catal.* **70**, L15 (1991).
4. Yokoyama, C., and Misono, M., *J. Catal.* **150**, 9 (1994).
5. Cowan, A. D., Cant, N. W., Haynes, B. S., and Nelson, P. F., *J. Catal.* **176**, 329 (1998).
6. Zuzaniuk, V., Meunieer, F. C., and Ross, J. R. H., *Chem. Commun.* 815 (1999).
7. Lombardo, E. A., Sill, G. A., d'Itri, J. L., and Hall, W. K., *J. Catal.* **173**, 440 (1998).
8. Beutel, T., Adelman, B., and Sachtler, W. M. H., *Catal. Lett.* **37**, 125 (1996).
9. Obuchi, A., Wögerbauer, C., Köppel, R., and Baiker, A., *Appl. Catal. B* **19**, 9 (1998).
10. Ukisu, Y., Sato, S., Muramatsu, G., and Yoshida, K., *Catal. Lett.* **11**, 177 (1991).
11. Li, C., Bethke, K. A., Kung, H. H., and Kung, M. C., *J. Chem. Soc. Chem. Commun.* 813 (1995).

12. Shimizu, K., Kawabata, H., Maeshima, H., Satsuma, A., and Hattori, T., *J. Phys. Chem. B* **104**, 2885 (2000).
13. Radtke, F., Koeppel, R. A., and Baiker, A., *Catal. Lett.* **28**, 131 (1994).
14. Radtke, F., Koeppel, R. A., and Baiker, A., *J. Chem. Soc. Chem. Commun.* 427 (1995).
15. Radtke, F., Koeppel, R. A., Minardi, E. G., and Baiker, A., *J. Catal.* **167**, 127 (1997).
16. Hamada, H., Kintaichi, Y., Sasaki, M., Ito, T., and Tabata, M., *Appl. Catal.* **64**, L1 (1990).
17. Hamada, H., *Catal. Surv. Jpn.* **1**, 53 (1997).
18. Akaratiwa, S., Nanba, T., Obuchi, A., Okazaki, J., Oi-Uchisawa, J., and Kushiyama, S., *Top. Catal.* **16/17**, 209 (2001).
19. Yogo, K., Umeno, M., Watanabe, H., and Kikuchi, E., *Catal. Lett.* **19**, 131 (1993).
20. Buckley, G. D., and Scaife, C. W., *J. Chem. Soc.* 1471 (1947).
21. Nanba, T., Obuchi, A., Izumi, H., Sugiura, Y., Zu, J., Uchisawa, J., and Kushiyama, S., *Chem. Commun.* 173 (2001).
22. Shamov, A. G., and Khrapkovskii, G. M., *in* "30th International Annual Conference ICT," p. 60-1. Karlsruhe, Germany, 1999.
23. Ugalde, J. M., *J. Mol. Struct. Theochem.* **258**, 167 (1992).
24. Dümpelmann, R., Cant, N. W., and Trimm, D. L., *J. Catal.* **162**, 96 (1996).
25. Chang, C. D., Hellring, S. D., and Pearson, J. A., *J. Catal.* **115**, 282 (1989).
26. Kiovsky, J. R., Koradia, P. R., and Lim, C. T., *Ind. Eng. Chem. Prod. Res. Dev.* **19**, 218 (1980).
27. Kleemann, M., Elsener, M., Koebal, M., and Wokaun, A., *Ind. Eng. Chem. Res.* **39**, 4120 (2000).
28. Nanba, T., Obuchi, A., Akaratiwa, S., Liu, S., Uchisawa, J., and Kushiyama, S., *Chem. Lett.* 986 (2000).
29. Goodman, A. L., Underwood, G. M., and Grassian, V. H., *J. Phys. Chem. A* **103**, 7217 (1999).
30. Richter, M., Eckelt, R., Parlitz, B., and Fricke, R., *Appl. Catal. B* **15**, 129 (1998).
31. Delahay, G., Coq, B., Kieger, S., and Neveu, B., *Catal. Today* **54**, 431 (1999).
32. Centi, G., Perathoner, S., Biglino, D., and Giamello, E., *J. Catal.* **151**, 75 (1995).